Colloid Polym Sci 276:109–116 (1998)

ORIGINAL CONTRIBUTION

M.G. Bonicelli
G.F. Ceccaroni
C. La Mesa

Lyotropic and thermotropic behavior of Alkylglucosides and related compounds

Received: 15 May 1997
Accepted: 08 September 1997

C. La Mesa (✉)
Dipartimento di Chimica
Universitá "La Sapienza"
Roma, Italia

M.G. Bonicelli
Dipartimento I.C.M.M.P.M.
Universitá "La Sapienza"
Roma, Italia

G.F. Ceccaroni
Dipartimento Tecnol. Chimiche
Universitá "Tor Vergata"
Roma, Italia

Abstract The phase diagram of the binary system composed of octyl-β-D-glucopyranoside and water was investigated and the phase boundaries were determined. Polarising optical microscopy was used to define the different phases, proton and deuterium NMR experiments to define the region of existence of the different phases and to obtain information on axiality and head group solvation. DSC experiments were performed to determine the thermal transitions from solid to thermotropic liquid crystals for octyl-β-D-gluco-pyranoside, the related alkylglucosides or maltosides, and to gain information on the role played by sugar units in the thermodynamics of such phase transitions.

Key words: Surfactants – alkylglucosides – phase equilibria – micelles – lyotropic liquid crystals – thermotropic liquid crystals.

Introduction

The discovery of the mesomorphic behavior is strictly related to studies on alkylated carbohydrates. On analysing the extracts from tuberculosis bacteria Koch observed unusual optical textures of their aqueous dispersions [1], whereas Fischer observed double melting phenomena in dry alkylpryanosides [2]. These studies are considered the first contributions on lyotropic and thermotropic behavior, respectively.

Alkyl glucosides (AGs) are known since long times and information is available on their thermotropic behavior [3, 4]. No efforts have been made to link the thermotropic and lyotropic properties, although these substances form micelles and lyotropic liquid crystals [5–10].

Concerning the polymorphic behavior of AGs in solution, the crystalline order in gels and solutions of N-octyl-gluconamide [9], the mesomorphic phases of N-alkyl lactosylamines [10] and the phase diagram of octyl-β-D-gluco pyranoside, OG, and of its thio homologue have been reported [7, 8]. The solution properties of OG have been previously reported and information on micelle formation and aggregate size, shape and hydration is available [8, 11–14]. Much less known are the solution properties of its homologues, but studies on solutions of octyl-thio-β-D-gluco-pyranoside, decyl-β-D-gluco-pyranoside, and decyl-β-maltoside have been recently performed [15].

Because of their molecular properties, the occurrence of an hydrogen-bond network between the sugar units is expected. It stabilizes the thermotropic phases and plays a role in lyotropic and solution phases. To clarify still open questions, we report on the phase equilibria for two alkyl glucosides, a structurally related thioglucoside and a maltoside.

Colloid & Polymer Science, Vol. 276, No. 2 (1998)

Experimental

Materials

Octyl-β-D-gluco-pyranoside, OG and octyl-thio-β-D-gluco-pyranoside, OTG, were from Sigma. Decyl-β-D-gluco-pyranoside, DG, and decyl-β-maltoside, DM, were from Fluka. They were free of surface active contaminants as inferred by surface tension versus log [m] plots: no downward inflections were observed at concentrations close to the CMC. The surfactants were dried, since weight losses were observed in thermogravimetric analysis (Table 1).

Contact with water vapour was avoided and the samples were stored over P_2O_5 until use.

Water was doubly distilled over alkaline $KMnO_4$, deionized and degassed: its specific conductance was $\approx 5 \times 10^{-7}\,\Omega^{-1}\,cm^{-1}$ at 298 K. Deuterium oxide, 99.8% isotopic enrichment, Merck, was used as such.

The samples were weighed in glass vials, flame sealed and centrifuged before and after sealing. They were kept inside an air oven at $\approx$ 400 K for some days, centrifuged back and forth (at 6000 rpm) until no bubbles or macroscopic inhomogeneities were observed and stored in a refrigerator at 263 K until use.

In isoplethal mode the samples were left to equilibrate at the required temperature for some minutes, to reduce the uncertainty in the phase boundaries. Phase transition temperatures were determined on heating.

Samples investigated by NMR were prepared by weight in 8 mm ∅ glass tubes and water was totally replaced by deuterium oxide on a mole fraction basis. Samples investigated by ^2H NMR contained $\approx$ 50 mg of D_2O per gram of sample.

The dry surfactants investigated by DSC were weighed in aluminium panels, which were immediately sealed.

Methods

Optical microscopy experiments were performed by a Leitz Laborlux polarizing microscope, connected to a Kofler hot stage, and by a CETI Topic microscope (Antwerp, Belgium) equipped with a CETI heating unit. In the latter case the working temperature is between 290 and 350 K and the accuracy $\pm$ 0.2 K. Details of the experimental set-up and measuring procedures are reported elsewhere [16].

Conoscopic investigations were also performed. The recognition of anisotropic textures was made according to Rosevear [17].

Visual inspection was performed by a home-made unit, with adjustable polarizer crossing, or by a thermostatic glycerol bath equipped with crossed polaroid windows.

Some samples were investigated by the penetration technique [18]. For this purpose small amounts ($\approx$ 30–50 mg) of the pure surfactant were put into thin glass tubes, melted and centrifuged. The waxy solid obtained from the above procedure was put under the microscope and some water (10–50 mg) was stratified by a microsyringe. The tubes were sealed and allowed to equilibrate at a given temperature for some minutes: the different optical textures indicate the phase sequence.

In penetration techniques, long-lasting measurements and scan of the phase sequence at different temperatures were avoided. The difference between phase boundaries obtained on individual samples and by penetration techniques is $\approx$ 3–5 K.

Solidus lines at moderate surfactant content were determined by cryoscopy, on a Knauer unit, equipped with a digital readout. Details of the apparatus set-up and the measuring procedures are reported elsewhere [12].

To determine the $l_1' \rightarrow L_1$ phase transition temperatures glass tubes for haematology were sealed at one tip and placed on the top of the liquid crystalline sample. The

Table 1 Thermal dehydration of glucoside surfactants from DTA thermograms

Weight % loss	Temperature range (K)	Weight % loss	Temperature range (K)
Octyl-β-D-glucoside		Octyl-thio-β-D-glucoside	
0.18 (± 0.01)	313–343	0.22 (± 0.02)	313–343
0.93 (± 0.03)	338–373	1.03 (± 0.05)	338–373
1.13 (± 0.05)	338–423	1.33 (± 0.07)	338–423
97.90 (± 0.15)*	423–673		
Decyl-β-D-glucoside		Decyl-β-maltoside	
0.20 (± 0.03)	313–343	0.32 (± 0.04)	313–343
0.98 (± 0.03)	338–373	1.43 (± 0.05)	338–373
1.18 (± 0.06)	338–423	2.47 (± 0.11)	338–423

* Decomposes at 591 K

whole system was heated at the rate of 1–2 K min^{-1}. At the transition temperature, the small tubes penetrated into the sample: the accuracy on the transition temperatures is $\pm$ 2 K.

Deuterium quadrupole splittings were measured on a Brucker WM 300, between 285 and 370 K. Typical experimental conditions are: transient number 2.000, acquisition time 50 ms, number of pulses 400, pulse width 22 μs. Further details on the measuring procedures have been given elsewhere [16]. ^2H quadrupole splittings, Δ, in Hz, are the distances between two adjacent peaks; the accuracy of Δ values is to $\pm$ 3%. They were fitted into a general equation, which assumes water molecules to be rotationally and translationally free, or bound to different binding sites, according to [19]

$$\Delta = |P_b S_b \xi_b| \,, \tag{1}$$

where P_b, S_b and ξ_b indicate the relative weight of deuterium nuclei in a given binding site, the related bond order parameter and the quadrupole coupling constant of bound water molecules, respectively. In Eq. (1) rotationally free water has zero bond order parameter.

For symmetry reasons, the bond order parameter of water deuterons in lamellar phases is twice the value in the corresponding hexagonal phases [20]. Deuterium NMR spectra indicate that two-phase regions are narrow.

Conditions for performing proton and carbon NMR are reported elsewhere [16].

DTA experiments were performed by a TC10-TA unit, Mettler. The heating rate was 10 K min^{-1} and the air stream flow 100 ml min^{-1}. Data are reported in Table 1 and a DTA scan in Fig. 1.

DSC experiments were run on a Perkin-Elmer calorimeter, mod. DSC 4, whose measuring vessel is thermostated in controlled N_2 gas stream.

Thermal scans were performed at 0.5, 1.0, 3.0, 5.0 and 10 K min^{-1}. At 3 K min^{-1} speed the combined uncertainty on transition temperatures and heat effects is at a minimum. Data obtained by DSC are reported in Table 2.

Thermal hysteresis was observed in solid–liquid crystal phase transitions and transition temperatures were different in heating and cooling mode [21]. As expected, the heat involved in the liquid–liquid crystal phase transitions changes its sign on reverting the scan rate, as indicated in Fig. 2.

Results

Thermotropic behavior

The transition temperatures and enthalpies of the dry surfactants are reported in Table 2 and in Fig. 2. Data are consistent with literature findings [3, 22]. The uncertainty of T values is 2–3 K, depending on heating rates. T values in Table 2 were measured at the maximum amplitude, provided no peak overlapping occurs: otherwise, they were obtained by signal deconvolution, according to standard procedures. In this way, the small satellite wings occurring below and above the liquid crystal melting temperature of DG, reported in Table 2, have been resolved.

The melting temperature of dry surfactants, $T_{s,lc}$, is the upper limit of the gel to lamellar phase transition. The enthalpies of liquid crystal melting, $\Delta H_{lc,m}$, at the clearing point, T_c, are in the range 1–2 kJ mol^{-1}. Solid–liquid

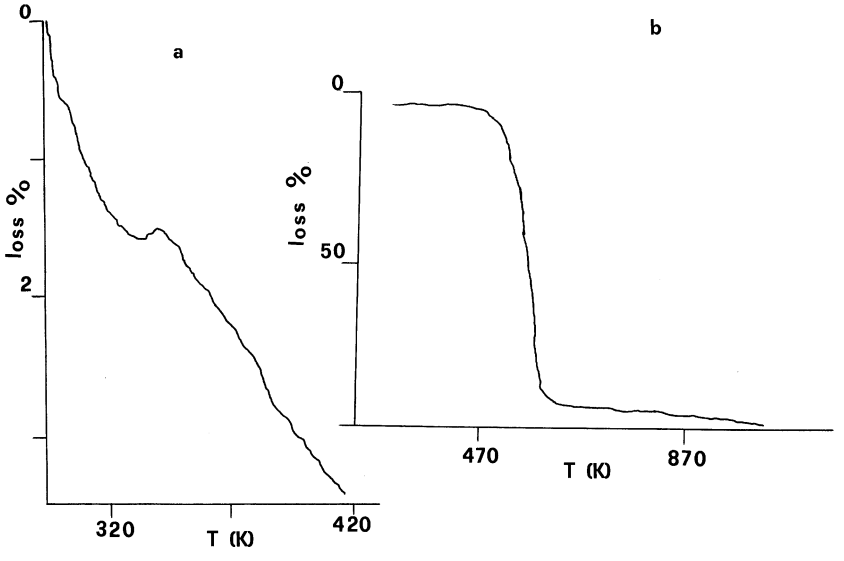

Fig. 1 DTA thermogram of OG in the range 310–420 K, (A) and 310–870 K, (B) Data are reported as wt% loss versus temperature

Colloid & Polymer Science, Vol. 276, No. 2 (1998)

Table 2 Transition temperatures and enthalpies of dry OG, OTG, DG and DM, obtained by DSC

T (K)	ΔH (kJ mol^{-1})	T (K)	ΔH (kJ mol^{-1})
Octyl-β-D-glucoside		Octyl-thio-β-D-glucoside	
324.8	0.4 (pretransition)	312.5 ($\pm$ 0.4)	30.9 (pretransition)
		312.9	20.3 (pretransition)
327.7	0.2 (pretransition)	403.6	1.8 (solid–liq. cryst.)
332.3	10.8 (solid–liq. cryst.)	478 ($\pm$ 2)	13.6 (liq. cryst. melting)
371.9 ($\pm$ 0.5)	1.2 (liq. cryst. melting)		
Decyl-β-D-glucoside		Decyl-β-maltoside	
317.3	13.1 (pretransition)	351.7 ($\pm$ 0.8)	10.9 (pretransition)
337.7	0.88	369.6	9.3 ($\pm$ 1.5) (solid–liq. cryst.)
347.7	−0.08		
349.0	8.59 (solid–liq. cryst.)		
363.3	0.12		
408.6			
409.8 ($\pm$ 1)	1.71 (liq. cryst. melting)	476 ($\pm$ 2)	1.1 (liq. cryst. melting)
415.9			

Note: Scan rates of 3 K min^{-1}. Unless, otherwise reported, the uncertainty in temperatures is $\pm$ 0.2 K. The uncertainty in enthalpies is $\pm$ 10% and $\pm$ 5% below and above 2 kJ mol^{-1}, respectively

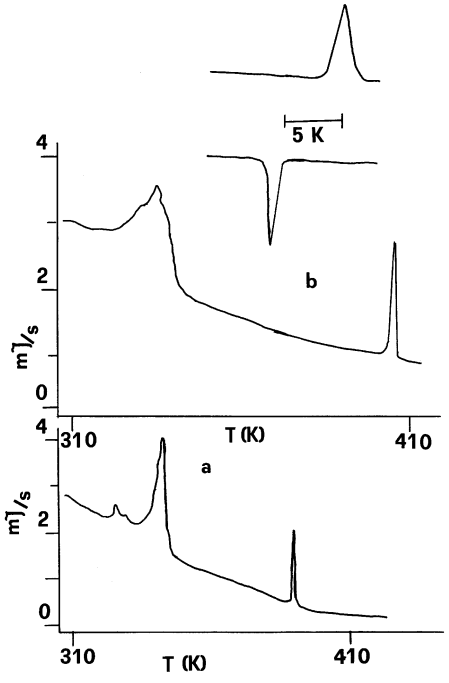

Fig. 2 DSC thermograms of OG, (A), and DG, (B). The scan rate is 3 K min^{-1}. In the inset is reported the inversion phenomenon observed on heating, (up), and cooling, (down), pure OTG. Temperatures are in Kelvin

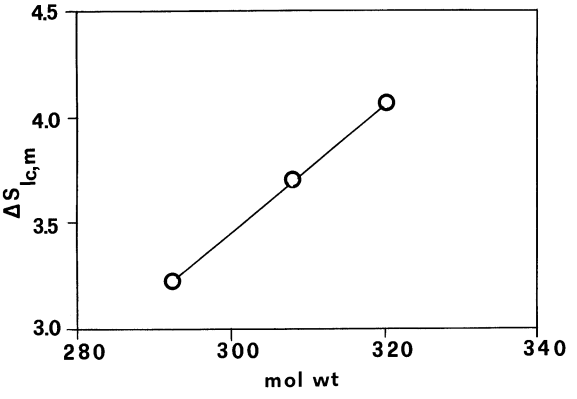

Fig. 3 Plot of $\Delta S_{lc,m}$, in J K^{-1}, versus the surfactant molecular weight

crystal transition enthalpies, $\Delta H_{s,lc}$, at $T_{s,lc}$, are close to 10 kJ mol^{-1}, with the only exception of OTG, $\approx$ 30 kJ mol^{-1}. No relation has been found between ΔH_{tr}, or $T_{s,lc}$ values and alkyl chain length. However, a plot of the entropy of melting $\Delta S_{lc,m}$, versus the monoglucoside molecular weight gives a straight line, Fig. 3.

A large thermal hysteresis is associated with these phase transitions. In some cases it is possible to keep the thermotropic melts at room temperature for several minutes, without occurrence of crystallisation: such an effect is significant in OG and OTG.

Information from polarising microscopy confirms DSC findings. No discontinuities were observed in the transitions from thermotropic to lyotropic phases, in accordance with studies on fatty acid soaps [23]. In particular, the anisotropic textures observed in the melts are similar to those observed in the adjacent lyotropic phases. Despite their optical activity, no cholesteric textures were observed.

Lyotropic behavior

The complete phase diagram of the water/OG system is reported in Fig. 4. The phase denomination, due to Ekwall [24], does not refer to any structural detail and is based on the "ideal" phase sequence of surfactant–water systems [25, 26].

The phase diagram was drawn by combining information from cryoscopy, visual observation, optical polarising microscopy, penetration techniques and ^{2}H NMR: the latter method gives information on the coexistence of different phases (provided the signals of water deuterons are strong and do not overlap), water binding and other effects, which will be considered later.

The phase diagram is very similar to that reported by Sakya [7] and Nilsson [8]. On increasing the surfactant content, at room temperature, the phase sequence is: solution region, L_1; hexagonal mesophase, H; viscous isotropic phase, I'_1; and lamellar phase, L. In isoplethic mode the thermal transitions from liquid crystal to solution phases were determined (Fig. 5). In particular, the presence of two phase regions can be inferred from the coexistence of splitting and single lines (due to the solution) in the spectrum of water deuterons.

The solution region extends up to about 60 wt% of surfactant and samples are characterised by a progressive increase of apparent viscosity. OG micelles are not spherical even at concentrations far from the phase boundaries [11, 14]. Support to this hypothesis came from the line broadening of proton NMR, ascribed to the progressive growth of anisometric micelles (Fig. 6). Surfactant self-diffusion has been interpreted by assuming that OG micelles are rods of small axial ratios [8], in agreement with viscosity [11, 14] and heat capacity data [12].

The hexagonal mesophase exhibits fanlike textures in optical polarising microscopy and well developed deuterium powder spectra. The temperature range where the H phase exists is small, compared with other surfactants. Its location in the phase diagram and the absence of a cubic phase between the solution phase and the mesophase support the hypothesis of micellar anisometry.

The viscous isotropic mesophase, I'_1, is located between the hexagonal and the lamellar one. At moderately high temperatures, it is in equilibrium with the micellar solution: at still higher temperatures, it merges into the solution. The samples are stiff and transparent. They give well developed proton NMR spectra (Fig. 6). The chemical environment sensed by OG molecules in this phase is not much different from the solution one: unfortunately, NMR spectroscopy does not give direct information on the self organisation of OG molecules in that phase [27, 28].

Fontell discussed the structures of viscous isotropic phases and suggested that they are not always formed by

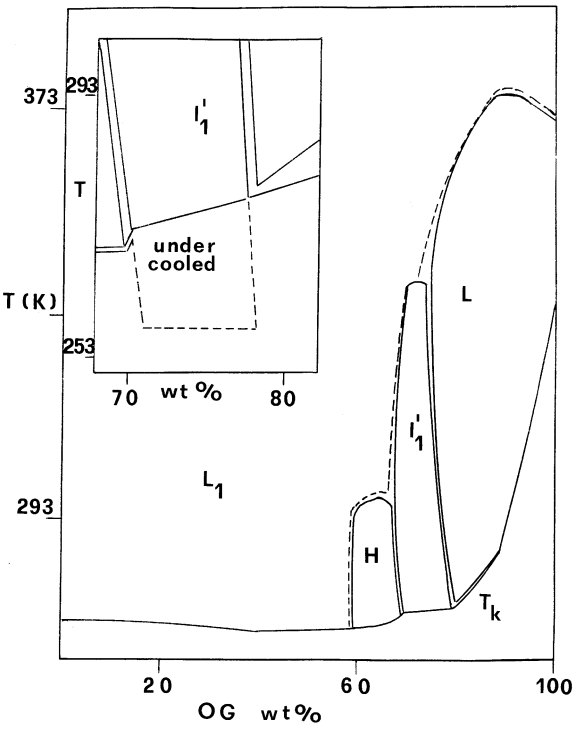

Fig. 4 Phase diagram of the system water/octyl-β-D-glucopyranoside, OG. The symbols mean the following: L_1, solution phase; H, hexagonal phase; I'_1, viscous isotropic phase; L, lamellar phase. The region below the T_k line represents solid (gel) phases. The amplitude of the two phase regions was inferred from the occurrence in NMR deuterium spectra of splittings and isotropic lines; in the cubic phase the uncertainty on phase boundaries is related to the accuracy in the determination of the fusion temperature, described in the experimental section. In the inset are reported the boundaries of the I'_1 phase on heating, full, and cooling, dotted line. The cooling rate is 2 K per hour

spherical units arranged in a cubic array. Accordingly, the interactions can be averaged, or not, depending on the space group [29], and the spectral lines large or narrow. The occurrence of quadrupolar effects in NMR spectra of such phases is controlled by the aggregate structure and axiality [30, 31]. In the present case no such effects were observed. If links between the location in the phase diagram and microscopic structure are accepted, the viscous isotropic phase should be bicontinuous, i.e. oil and water-continuous [32]. The Ia3d crystallographic structure, observed by X-ray scattering [7, 8], is in accordance with the present hypothesis.

A spectacular effect is the possibility of cooling viscous isotropic samples well below 0 °C, without phase separation, inset in Fig. 4. The kinetics of phase separation requires long equilibration times (over three weeks). This is in line with the statement that isotropic mesophases may be "pseudo-stable for a very long time at non-equilibrium

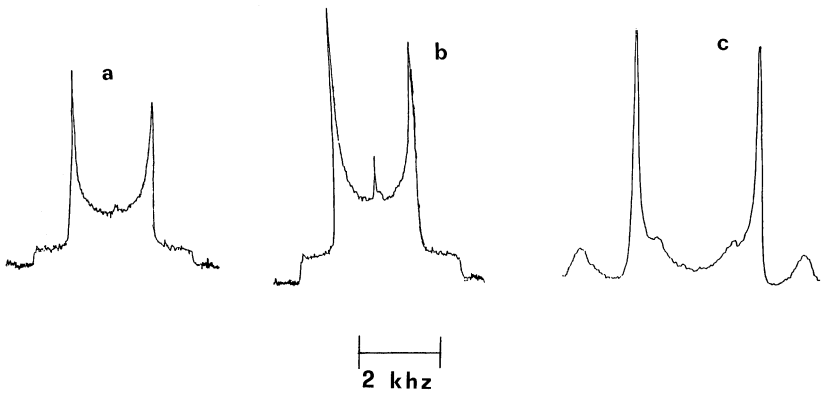

Fig. 5 Temperature dependence of deuterium quadrupole splittings, in KHz, at 291 K (a), and 293 K, (b) for a sample containing 59.2 OG wt%, H phase. At 296 K the quadrupole splitting disappears. In (c) is reported the spectrum of a sample containing 84.7 OG wt%, at 313 K, showing the occurrence of a second weak splitting

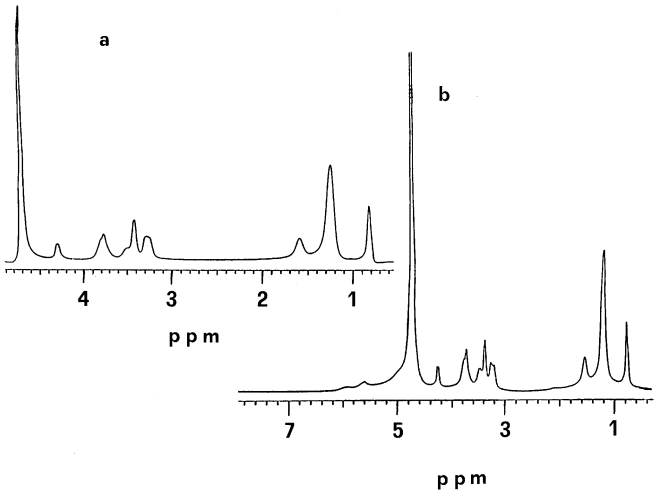

Fig. 6 Proton NMR spectra of 0.56 molal OG solution in D_2O (a), and of a sample in the viscous isotropic phase (b), containing 74.1 OG wt%, at 298 K

temperatures" [29]. Such effect might be important in technological applications, for instance, in enzyme trapping and in biochemically relevant processes.

The lamellar phase extends up to the solid phase, or thermotropic melt, depending on temperature and composition. In polarised light it shows oily streaks and mosaic textures: it was not possible to distinguish the textures of the thermotropic melt from those of the lyotropic phase. At concentrations close to the gel–liquid crystal solidus line, the occurrence of a (S_1, $C = \pi/2$) disclination [33] was observed. We do not know the reasons for such a behavior, presumably due to the nucleation of solid crystallites into a lamellar domain.

A comparison between the phase behavior of OG and glucosides was tentatively made by penetration techniques. In the water–OTG system, at room temperature the observed phase sequence was $L_1 \rightarrow I'_1 \rightarrow L$, in line with previous studies [7]. In this system a thermal transition from cubic to lamellar phase occurs.

DG does not form cubic, or hexagonal, phases. The width of the solution region is difficult to quantify and experimental evidence on the occurrence of turbid, presumably biphasic, region was obtained. DM forms hexagonal and lamellar phases, separated by an optically transparent region.

Discussion

The mesomorphic behavior of aqueous surfactant systems is controlled by their optimal alkyl chain length, volume and area per polar head group. The phase sequence follows the requirements dictated by the R theory [25] and/or by the packing-constraint one, PC [34]. Such theories take into account the average interfacial properties and those of the individual components, respectively. In both cases the lamellar phase is assumed as a reference state, because of its zero interfacial curvature. Not all phase transitions are observed in a given system and information on the forces driving the surfactant self organization can be inferred from a comparison of experimental and predicted trends.

The polar head group plays an important role in the polymorphic behavior of lyotropic phases. The interactions between water and polar heads depend on the surfactant molecular properties and slight variations control the phase sequence [35, 36]. Alkylglucosides have bulky sugar residues as polar head, with many hydroxyl groups facing toward the water pool. The formation of hydrogen bonds between glucosides and water, or between adjacent amphiphilic molecules, does not afford a significant compression and/or desolvation of the area per polar head groups.

In anisotropic phases nuclei with spin quantum number $l \geqslant 1/2$ split their signal into $2l$ lines, because the

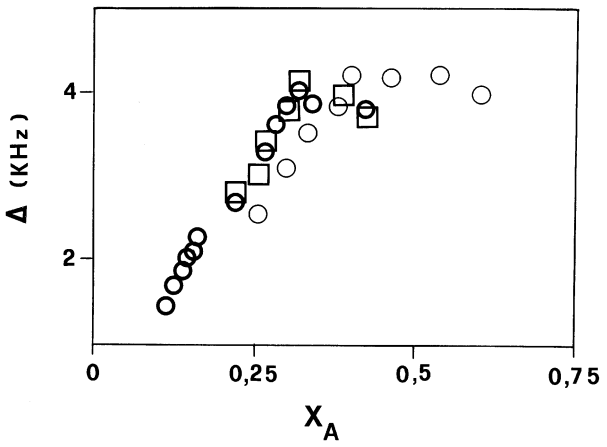

Fig. 7 Dependence of deuterium quadrupole splittings, Δ, in kHz, on the surfactant mole fraction, X_A, in the lamellar and hexagonal (thick circles) phase of OG, and in the lamellar phase of DG, (circles), and OTG, (squares), at 293 K

non-averaged molecular (or aggregate) motion gives rise to residual interactions, with occurrence of static effects [20]. In the samples we have investigated, no biaxial character was found. In the lamellar phase the relation between quadrupole splittings and mole fraction has a slope higher than that in the hexagonal phase [37], Fig. 7.

Information on average hydration numbers in lyotropic phases was inferred by fitting the deuterium quadrupole splittings in a two-site approximation of Eq. (1), according to

$$\Delta = [\langle n\rangle X_a/(1 - X_A)]S_b\xi_b\,, \qquad (1')$$

where X_A is the surfactant mole fraction, S_b the order parameter of bound water (≈ 0.01) and $\langle n\rangle$ the average hydration number per surfactant molecule. ξ_b is ≈ 220 kHz. In Fig. 7 the quadrupole splittings are reported versus the surfactant mole fraction, X_A, to have information on hydration.

For water–OG mixtures in H phase, hydration numbers are 6–8 per surfactant unit and 10–12 in the water–DM system. In the corresponding lamellar phases, they are 4 ± 1.5 and 7 ± 2, respectively. Hydration numbers of OG in the H phase are close to those inferred from dielectric relaxation spectroscopy in concentrated micellar solutions [14]. In the lamellar phase, the hydration numbers of OTG. OG and DG are very close to each other. Thus, the average hydration numbers per sugar unit are nearly constant in a given phase.

Information on the role of hydrogen bonds in the stabilization of such phases can be inferred from deuterium spectral profiles, Fig. 5. For instance, at OG content higher than 80 wt%, the quadrupole splitting is nearly constant and a second weak splitting is observed: its location is nearly independent of composition. Such effects can be related to the bond order parameters of ^2H nuclei in the sugar unit and to interactions between them. In fact, the resonance lines are broader than those of bound water. Similar effects have been observed in DG and, to a much lower extent, in DM, but not in OTG. This is in agreement with the current knowledge on packing in monolayers: in particular, the sugar units bound to a sulphur atom do not pack in close form, because of the high sterical hindrance of sulphur with respect to oxygen [7].

Conclusions

Information on hydration and thermal stability of the different phases was given for some glucosides and maltosides: it can be extended to cerebrosides [38, 39]. As to the thermotropic behavior, attempts to give account of the properties of α and β anomers, to obtain information on the relations between phase properties and head group conformation [40], are in progress.

Acknowledgements CNR, the Italian National Research Council, is acknowledged for financial support. We thank Prof. Mauro Tomassetti, "La Sapienza", Rome, for allowing us the use of his DTA unit.

References

1. Koch R (1884) Mitt K Gesundheitsamt 2:1
2. Fischer E, Helferich B (1911) Justus Liebigs Ann Chem 383:68
3. Jeffrey GA (1986) Acc Chem Res 19:168
4. Denkinger P, Kunz M, Burchard W (1990) Colloid Polym Sci 268:513
5. Warr GG, Drummond CJ, Grieser F, Ninham BW, Evans DF (1986) J Phys Chem 90:4581
6. Platz G, Pölike J, Thunig C, Hofmann R, Nickel D, von Rybinski W (1995) Langmuir 11:4250
7. Sakya P, Seddon JM, Templer RH (1994) J Phys II (Paris) 4:1311
8. Nilsson F, Söderman O, Johansson I (1996) Langmuir 12:902
9. Svenson S, Köning J, Fuhrhop JH (1994) J Phys Chem 98:1022
10. Auvray X, Petipas C, Anthore R, Rico-Lattes I, Lattes A (1995) Langmuir 11: 433
11. La Mesa C, Bonincontro A, Sesta B (1993) Colloid Polym Sci 271:1175
12. Antonelli ML, Bonicelli MG, Ceccaroni GF, La Mesa C, Sesta B (1994) Colloid Polym Sci 272:704
13. D'Aprano A, La Mesa C, Proietti N, Sesta B, Tatone S (1994) J Solution Chem 23:106
14. Bonincontro A, Briganti G, D'Aprano A, La Mesa C, Sesta B (1996) Langmuir 12:3206

15. Decina Di Pirro MR (1996) Thesis, La Sapienza University, Rome
16. La Mesa C, Sesta B, Bonicelli MG, Ceccaroni GF (1990) Langmuir 6:1662
17. (a) Rosevear FB (1954) J Am Oil Chem Soc 31:620. (b) Rosevear FB (1968) J Soc Cosm Chem 19:581
18. Rendall K, Tiddy GJT, Trevethan M (1983) J Chem Soc Faraday Trans I 79:637
19. Wennerström H, Lindblom G, Lindman B (1974) Chem Scripta 6:97
20. Wennerström H, Persson NO, Lindman B (1976) Am Chem Soc Symp Ser 34:372
21. Goodby JW (1984) Mol Cryst Liq Cryst 110:205
22. Dorset DL, Rosenbusch JP (1981) Chem Phys Lipids 29:299
23. McBain JW, Lazarus LH, Pitter AV (1930) Z Phys Chem (Leipzig) 147:87
24. Ekwall P (1975) In: Brown GH, (ed) Advances in Liquid Crystals. Academic Press, New York, Vol I, p 1
25. Winsor PA (1968) Chem Rev 68:1
26. Tiddy GJT (1980) Phys Rep 57:1
27. Charvolin J, Rigny P (1969) J Physique (Paris) C4:30
28. Lindblom G, Wennerström H (1977) Biophys Chem 6:167
29. Fontell K (1990) Colloid Polym Sci 268: 264
30. Söderman O, Walderhaug H, Henriksson U, Stilbs P (1985) J Phys Chem 89: 3639
31. Söderman O, Henriksson U (1987) J Chem Soc Faraday Trans I 83: 1515
32. Fontell K (1982) Mol Cryst Liq Cryst 63: 59
33. Chandrasekhar S (1977) In: Liquid Crystals. Cambridge University Press, Cambridge, Chap. III, p 126
34. Zhang K, Lindman B, Coppola L (1995) Langmuir 11:538
35. Israelachvili JN, Mitchel DJ, Ninham BW (1976) J Chem Soc Faraday Trans II 72:1525
36. Evans DF, Ninham BW (1986) J Phys Chem 90:226
37. Jönsson B, Wennerström H (1987) J Phys Chem 91:338
38. (a) Luzzati V (1968) In: Chapman D (ed) Biological Membranes. Academic Press, New York, p 71; (b) Luzzati V, Gulik-Krzywicki T, Tardieu A (1968) Nature 218:1031.
39. Curatolo W, Jungalwala FB (1985) Biochemistry 24:6608
40. Jeffrey GA, Bhattacharjee S (1983) Carbohydr Res 115:53